Journal of Alloys and Compounds 688 (2016) 1157–1161

Contents lists available at ScienceDirect

Journal of Alloys and Compounds

journal homepage: http://www.elsevier.com/locate/jalcom

Sol – gel synthesis, structural characterization and bifunctional catalytic activity of nanocrystalline delafossite $CuGaO_2$ particles

Jahangeer Ahmed [a, *], Viktor V. Poltavets [b], Jai Prakash [c], Saad M. Alshehri [a], Tansir Ahamad [a]

[a] Department of Chemistry, College of Science, King Saud University, Riyadh, 11451, Saudi Arabia
[b] Department of Chemistry and Advanced Materials Research Institute, University of New Orleans, New Orleans, LA, 70148, USA
[c] Department of Chemistry, Michigan State University, East Lansing, MI, 48824, USA

ARTICLE INFO

Article history:
Received 2 June 2016
Received in revised form
1 July 2016
Accepted 2 July 2016
Available online 9 July 2016

Keywords:
Sol – gel synthesis
$CuGaO_2$
Nanoparticles
Bifunctional catalyst

ABSTRACT

Nanoparticles of $CuGaO_2$ delafossite were successfully synthesized from the sol – gel process by controlling the atmospheric conditions at 850 °C. The average size of $CuGaO_2$ nanoparticles of ~40 nm was determined by transmission electron microscopy. Note that the thermodynamically stable conditions for $CuGaO_2$ delafossite synthesis are 1100 °C and 1200 °C in nitrogen and air atmosphere, respectively, while our methodology stabilizes the $CuGaO_2$ particles in the nano-metric region at low temperature (i.e. 850 °C). Moreover, delafossites $CuGaO_2$ nanoparticles show very interesting bifunctional catalytic activity in the electrolysis of water with O_2 and H_2 generation at anodic and cathodic potentials respectively. The current densities of $CuGaO_2$ nanoparticles as the bifunctional catalysts were found to be 15 mA/cm^2 and 18 mA/cm^2 for H_2 and O_2 generation, respectively, using 0.5 M KOH solution as an electrolyte versus Ag/AgCl electrode.

1. Introduction

Delafossite oxides have great potential as electro-catalysts [1–3], photo-catalysts [4–7], as well as electronic [7–9] and optical materials [8,9]. Delafossites are the ternary oxides with the general formula ABO_2, where 'A' is monovalent (e.g. Cu^+, Ag^+ etc) and 'B' is trivalent (Al^{3+}, Ga^{3+}, In^{3+}) cations [10,11]. Delafossite oxide ($CuGaO_2$) belongs to a group of p – type transparent conducting oxides (TCOs) and has direct and indirect band gap of 3.9 eV and 1.4 eV respectively [12–14]. The p – type conductivity in delafossites was revealed by Kawazoe et al. in 1997 for the first time [15]. In the last few years, photo-electrochemical properties of delafossite materials for solar cell applications were actively studied [6,16,17]. However, the detailed electrochemical studies of delafossites ABO_2 oxides are still needed. The present work displays very interesting bifunctional electro-catalytic activity of $CuGaO_2$ nanoparticles in electrolysis of water for H_2 and O_2 generations at cathode and anode respectively. In the last decade, substantial advances were made for enabling renewable and clean energy sources. The electrolysis of water can be a significant process for storing renewable energy as H_2 fuel, which can be transformed later into electricity by fuel cells.

Low temperature synthesis of delafossite oxides with controlled particle shape and size is challenging. Therefore, a portion of the present work is devoted to a development of a low temperature synthesis of the delafossites nanoparticles with controlled size. Except for a hydrothermal process, no other low temperature method was reported for the synthesis of $CuGaO_2$ nanoparticles. $CuGaO_2$ nanoplates were synthesized from the hydrothermal route and were used as the photo-electrocatalysts in p – type dye sensitized solar cells (DSSCs) [6]. Solid state route was employed to obtain the $CuGaO_2$ and indium doped $CuGaO_2$ particles at 975 °C. The performance of these particles was investigated as the photo-electrode materials for hydrogen generation via splitting of hydrogen sulfide (H_2S) in visible region [5]. Moreover, polycrystalline delafossite $CuGaO_2$ and iron doped $CuGaO_2$ materials were also synthesized by the solid state method at 1100 °C and were used in the photochemical reduction of CO_2 to CO [7]. It is not possible to synthesize delafossite $CuGaO_2$ below 1100 °C and 1200 °C in N_2 and air atmosphere respectively [18]. Therefore, since a high temperature annealing for $CuGaO_2$ solid state synthesis is required, the preparation leads to large micron size particles. The

* Corresponding author.
E-mail address: jahmed@ksu.edu.sa (J. Ahmed).

http://dx.doi.org/10.1016/j.jallcom.2016.07.017
0925-8388/

only publication on the hydrothermal preparation of $CuGaO_2$ nanoparticles reported the particle of 200–300 nm in size [6,19,20]. It is noteworthy that there is no report on the sol – gel synthesis of $CuGaO_2$ nanoparticles with controlled size. However, $CuGaO_2$ nanoparticles with the size less than 50 nm could be an ideal choice in the applications of energy conversion and conservation. Previously, several other ternary oxides like $CuAlO_2$, $BaSnO_3$, $SrSnO_3$ etc. have been synthesized by us using the low temperature methods and studied their respective properties [4,21].

Herein, we report the sol – gel synthesis of delafossite $CuGaO_2$ nanoparticles (~40 nm) by controlling the atmospheric conditions at 850 °C. The bifunctional electro-catalytic activity of delafossite $CuGaO_2$ nanoparticles has also been investigated with the help of three electrode electrochemical work station and this shows a significant impact on H_2 and O_2 generation from the electrolysis of water. Thermal stability of the $CuGaO_2$ nanoparticles in oxygen atmosphere has also been investigated. The structural and morphological characterizations of the nanoparticles were successfully investigated by powder X-ray diffraction (PXRD), thermogravimetric analysis and high resolution transmission electron microscopy (HRTEM).

2. Materials and methods

The following reagents were used in the sol – gel synthesis of $CuGaO_2$ nanoparticles: citric acid (Sigma Aldrich, 99.5+%), ethylene glycol (JADE scientific), $Cu(NO_3)_2 \cdot 2.5H_2O$ (Aldrich Chemical Company, 98%), $Ga(NO_3)_3 \cdot xH_2O$ (Alfa Aesar, 99.9%), and nitrogen gas (99.99%). Commercially available reagent, $Ga(NO_3)_3 \cdot xH_2O$, has six water molecules, which is produced by the weight loss of ~74% of reagent from the thermal analysis, as also reported [22]. The simple and inexpensive sol – gel process is an important tool for the preparation of a variety of nanostructured materials in large scale for numerous applications. An appropriate stoichiometric composition of copper and gallium compounds, in the ratio of 1:1 (0.1 M $Cu(NO_3)_2 \cdot 2.5H_2O$ and 0.1 M $Ga(NO_3)_3 \cdot 6H_2O$), were mixed together under constant stirring on a magnetic stirrer for 10 min. Afterward, the homogeneously mixed solution was transferred to a porcelain crucible containing 0.15 mol of anhydrous citric acid, 10 ml of ethylene glycol and 1 ml of concentrated nitric acid. A clear deep blue colored solution of Cu–Ga precursor was appeared immediately. The evaporation of water of Cu–Ga precursor took place at room temperature and turned in to the viscous gel after three days. This gel was kept for another three days at 300 °C and the brownish black colored condensed gel was obtained. The resulting condensed gel material was fired at 350 °C for 6 h in air, which lead to the formation of fine black powders. PXRD patterns primarily show the formation of copper (II) oxide and amorphous gallium based compound at 350 °C. The resulting fine black powders were then fired at 700 °C for 12 h in air resulting in the formation of CuO and $CuGa_2O_4$ followed by the palletization of the resulting powders and used as the final precursors in the synthesis of gray colored nanoparticles of delafossite $CuGaO_2$ at 850 °C for 48 h with the constant heating rate of 100 °C/h under the flow of highly pure nitrogen (99.99%) gas. Note that the above resulting $CuGaO_2$ nanoparticles were termed "CGO - 1" while term "CGO - 2" is used for the $CuGaO_2$ nanoparticles obtained by the process given below. The $CuGaO_2$ nanoparticles (i.e. CGO - 2) were also synthesized in a closed silica tubes using the same precursor materials under a controlled partial pressure of oxygen (i.e. $pO_2 = 10^{-5}$ atm) at 850 °C for 72 h.

PXRD studies were used to characterize the as - synthesized materials on a Bruker D8 Advance diffractometer with Ni-filtered Cu-Kα radiation with a scan speed of 1 s and scan step of 0.02°. Thermogravimetric (TGA) and differential scanning calorimetry (DSC) were carried out using a Perkin-Elmer system in flowing nitrogen gas, with a heating rate of 5 °C/min. HRTEM and TEM studies were carried out with a Technai G^2 20 electron microscope operated at 200 kV. The specimens for TEM were prepared by dispersing the powder sample in acetone by the ultrasonic process, and putting a drop of sample on a copper grid consisting of a porous carbon film, and then drying in air.

Bifunctional electro-catalytic activity has been studied with a computer controlled three electrode electrochemical work station (potentiostat/galvanostat, Metrohm Autolab B.V.) at 25 °C. Pt wire,

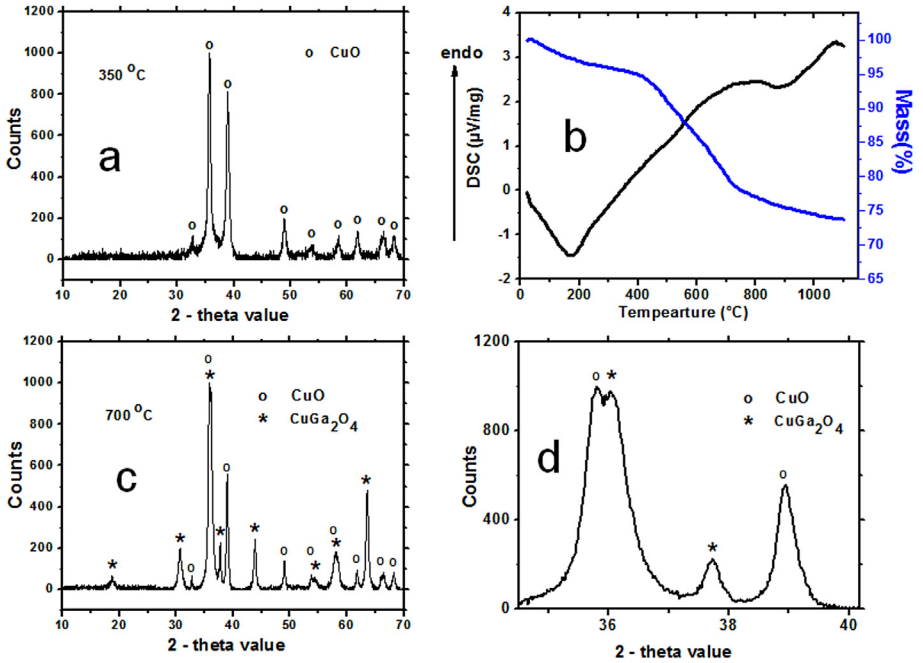

Fig. 1. (a) PXRD patterns of as - synthesized Cu-Ga precursor materials at 350 °C/6h/air, (b) TGA / DSC studies of the as synthesized Cu-Ga precursor materials at 350 °C/6h/air, (c) PXRD patterns of Cu-Ga precursor heated at 700 °C/12h/ air, and (d) x-ray line broadening studies of Cu-Ga precursor heated at 700 °C/12h/ air.

Ag/AgCl, and glassy carbon electrodes were used as the counter electrode, reference electrode and working electrode, respectively, in the electrolysis of water to H_2 and O_2 generation. The working electrodes were prepared by using the previously reported procedure [1]. Cyclic voltammetry (CV) was carried with the scan rate of 50 mV/s, and the peak windows between from −1.0 to 1.0 V versus Ag/AgCl electrode and from −1.2 to 0.0 V versus Ag/AgCl electrode using 0.5 M KOH as an electrolyte solution. Chrono-amperometric (CA) studies were carried out at 0.60 V and −1.2 V versus Ag/AgCl electrode for O_2 and H_2 generation, respectively, in 0.5 M KOH electrolyte solution. Note that N_2 gas was purged through the electrolyte solution for ~5 min before to start the electrochemical experiments. The purpose of flow of N_2 gas through the electrolyte solution was to remove the dissolved air from the electrolyte solution.

3. Results and discussion

PXRD studies primarily show the crystalline phase of copper (II) oxide and amorphous gallium based compound at 350 °C for 6 h in air (Fig. 1a). Thermal studies, of as synthesized materials at 350 °C, were carried out in the nitrogen atmosphere with the constant heating rate of 5 °C per minute which demonstrates a gradual weight loss from 400 °C to 800 °C, signifying the loss of oxygen molecules and organic moieties (Fig. 1b). The weight loss of Cu–Ga precursor could be ascribed the formation of delafossite $CuGaO_2$ in controlled atmosphere. However, no signal was observed in DSC curve around the transition temperature, which could be possible because of the slow kinetics of the reaction (Fig. 1b). Subsequently, heating of the materials at 700 °C for 12 h in air resulted in the formation of final precursor materials containing CuO and $CuGa_2O_4$ in 1:1 ratio without any organic moieties (Fig. 1c). A careful analysis of the intensity of the most prominent PXRD peaks of CuO and $CuGa_2O_4$ confirmed the 1:1 ratio of CuO and $CuGa_2O_4$ (Fig. 1d). The final precursor material was then fired at 850 °C under controlled atmospheric conditions (either flow of N_2 99.99% or controlled $pO_2 = 10^{-5}$ atm) and lead to the formation of pure phase delafossite $CuGaO_2$ nanoparticles.

Note that the bulk sized particles of $CuGaO_2$ are thermodynamically unstable at or below 1100 °C and 1200 °C in nitrogen and air respectively [18]. We agree with the previous report that small size and narrow size distribution of the particles plays the crucial role in the formation of pure $CuGaO_2$ nanoparticles at low temperature [18]. The final precursor materials were used in pellet form for the synthesis of the delafossite $CuGaO_2$ nanoparticles. The pellets were fired at 800 °C for 48 h with the heating rate of 100 °C/h under the flowing of pure nitrogen (99.99%) gas resulted in the formation of $CuGaO_2$ (70%) along with the impurities of $CuGa_2O_4$ (20%) and Cu_2O (10%). The pure phase of delafossite $CuGaO_2$ nanoparticles was obtained by subsequent firing at 850 °C for 48 h with a constant heating rate of 100 °C/h in highly pure N_2 atmosphere (Fig. 2a). The observed reflections of the delafossite $CuGaO_2$ nanoparticles from the powder X-ray diffraction studies could be indexed on the basis of rhombohedral unit cell with the space group R-3m (JCPDS file # 00-035-1402) and the refined lattice parameters were found to be 'a' = 2.9697 (4) and 'b' = 16.9525 (3) Å. The crystallite size of $CuGaO_2$ nanoparticles was also calculated from the line broadening studies using Scherrer's Formula; [$t = 0.9\lambda/(B \cos\theta)$], where; t, λ and B are the diameter of the particle, wavelength of Cu Kα radiation (1.5418 Å) and the line broadening respectively [23]. The crystallite size of $CuGaO_2$ nanoparticles was found to be 40 ± 5. Moreover, under the controlled partial pressure of oxygen of 10^{-5} atm, the delafossite $CuGaO_2$ nanoparticles were also synthesized at 850 °C for 3 days (by using the same precursor as discussed above) in a closed silica tube (Fig. 2b). Present studies show that the low partial pressure of oxygen of 10^{-5} atm may also lead the formation delafossite $CuGaO_2$ nanoparticle. Previously, Kumekawa et al. have reported the synthesis of micro-sized particles of $CuGaO_2$ using log $P(O_2)$ as low as − 4 [18].

Electron microscopic studies show the formation of delafossite $CuGaO_2$ nanoparticles with the small amount of agglomeration at 850 °C in the nitrogen atmosphere (Fig. 3a). The average size of the nanoparticles was found to be ~40 nm from the TEM studies, which is very close to the size obtained from X-ray line broadening studies. High resolution TEM studies showed the lattice fringes with d-spacing value of ~2.40 Å which agrees PXRD patterns with that of the plane <012> of the rhombohedral unit cell of delafossite $CuGaO_2$ nanoparticles (Fig. 3b). TEM studies also demonstrate the formation of the delafossite $CuGaO_2$ nanoparticles with an average diameter of ~45 nm at 850 °C using pO_2 of 10^{-5} atm (Fig. 3c). HRTEM studies of the delafossite $CuGaO_2$ nanoparticles show the d-spacing value of ~2.41 Å, which is consistent with that of the plane <012> of $CuGaO_2$ nanoparticles (Fig. 3d). Note that this is the smallest average size of the delafossite $CuGaO_2$ nanoparticles reported so far. Previously, hydrothermal method had been used for the synthesis of polycrystalline $CuGaO_2$ nanoparticle with the average particle size of ~200 nm [6,19,20].

We have re-investigated the thermal stability of the delafossite $CuGaO_2$ nanoparticles in oxygen atmosphere up to 1100 °C using the thermo-gravimetric analyzer (TGA) with the heating rate of

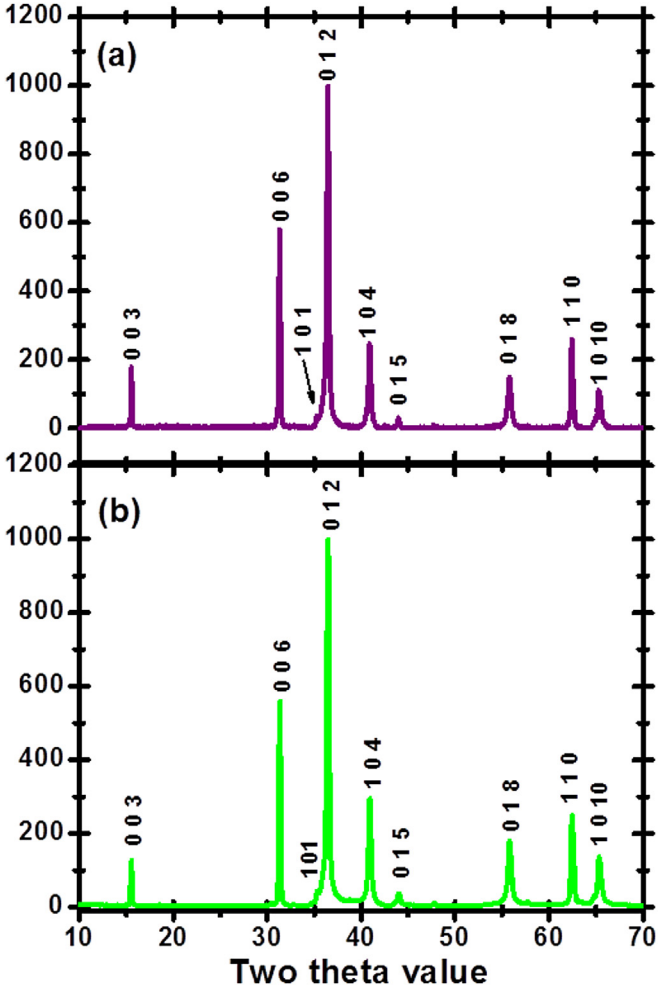

Fig. 2. PXRD studies of the delafossite $CuGaO_2$ nanoparticles obtained at (a) 850 °C/48 h/N_2 (termed as CGO - 1) and (b) 850 °C/72 h/$pO_2 = 10^{-5}$ atm (termed as CGO - 2).

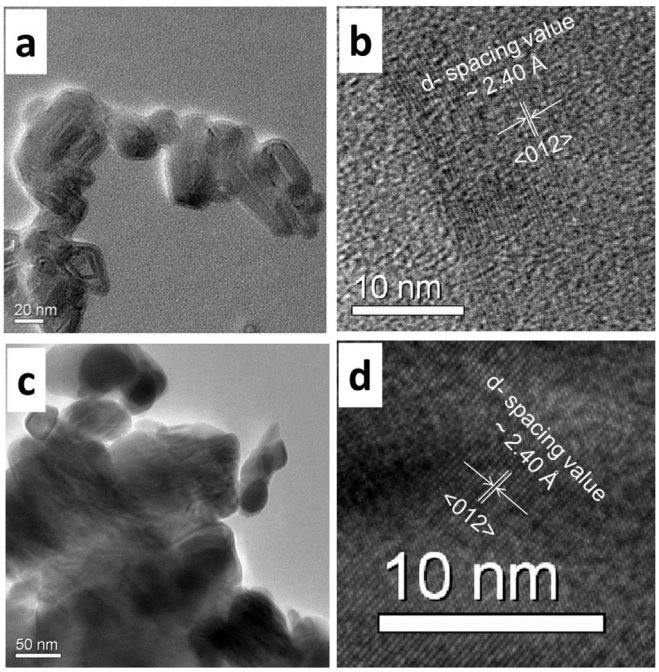

Fig. 3. (a) TEM and (b) HRTEM micrograph of the delafossite $CuGaO_2$ nanoparticles obtained at 850 °C/48 h/N_2 (CGO - 1). (c) TEM and (d) HRTEM micrograph of $CuGaO_2$ nanoparticles obtained at 850 °C/72 h/$pO_2 = 10^{-5}$ atm (CGO - 2).

5 °C/min. TGA studies confirmed that the delafossite $CuGaO_2$ nanoparticles are stable up to 350 °C in the oxygen atmosphere that show the lack of oxygen deficiency in the $CuGaO_2$ nanoparticles. The weight increase, from 350 °C to 700 °C of ~5%, is specified the decomposition of $CuGaO_2$ nanoparticles to CuO and $CuGa_2O_4$. The present results of thermal analysis of $CuGaO_2$ completely agree with earlier report [18]. Afterward, we observed a discontinuous mass decrease and an endothermic signal at 1050 °C, which could be concluded to reduction of CuO (i.e. Cu^{2+}) to Cu_2O (i.e. Cu^{+}).

Fig. 4 shows the cyclic voltammograms (CV) and CA studies of the nanocrystalline delafossite $CuGaO_2$ particles (CGO -1 and CGO - 2). Fig. 4a shows the CV curves of $CuGaO_2$ nanoparticles from −1.0–1.0 V versus Ag/AgCl with the scan rate of 50 mV/s. Purple and green colored CV curves belong to the sample CGO − 1 and CGO − 2 respectively. The CV curves exhibit the oxidation - reduction behavior and two very sharp peaks were appeared at −0.17 and −0.45 V, that resemble the oxidation of Cu to Cu^{+} and to Cu^{2+}, respectively, as reported earlier [24,25]. This is notable that the oxidation current was observed in CV beyond the potential of 0.55 V to O_2 generation in 0.5 M KOH according to the following reaction: $4OH^{-} \rightarrow 2H_2O + 2O_2 + 4e^{-}$ (at anode). From the CV curves (Fig. 4a), we observed that nanocrystalline $CuGaO_2$ particles (CGO - 1) generate slightly higher anodic current than nanocrystalline $CuGaO_2$ particles (CGO - 2) as well as CGO − 1 generate higher cathodic current than CGO − 2 according to the following reaction: $2H_2O + 2e^{-} \rightarrow H_2 + 2OH^{-}$ (Fig. 4b).

Potentiostatic quantitative measurements (chrono-amperometry (CA)) investigate the electro-catalytic activity of CGO − 1 and CGO - 2 at the fixed anodic and cathodic potential with time for O_2 and H_2 generation respectively. Fig. 4c shows the CA curve of CGO − 1 and CGO - 2 at the fixed anodic potential of 0.60 V for 25 s with multiple cycles for O_2 evolution reaction. By comparing the catalytic activity of both electrode materials with CA, we clearly observe that CGO - 1 has a higher current density (18 mA/cm^2) than CGO − 2 (13 mA/cm^2). A careful visualization of CA curves shows that the resulting current density of CGO − 1 is consistent with all cycles while the current density of CGO − 2 decreases with the number of

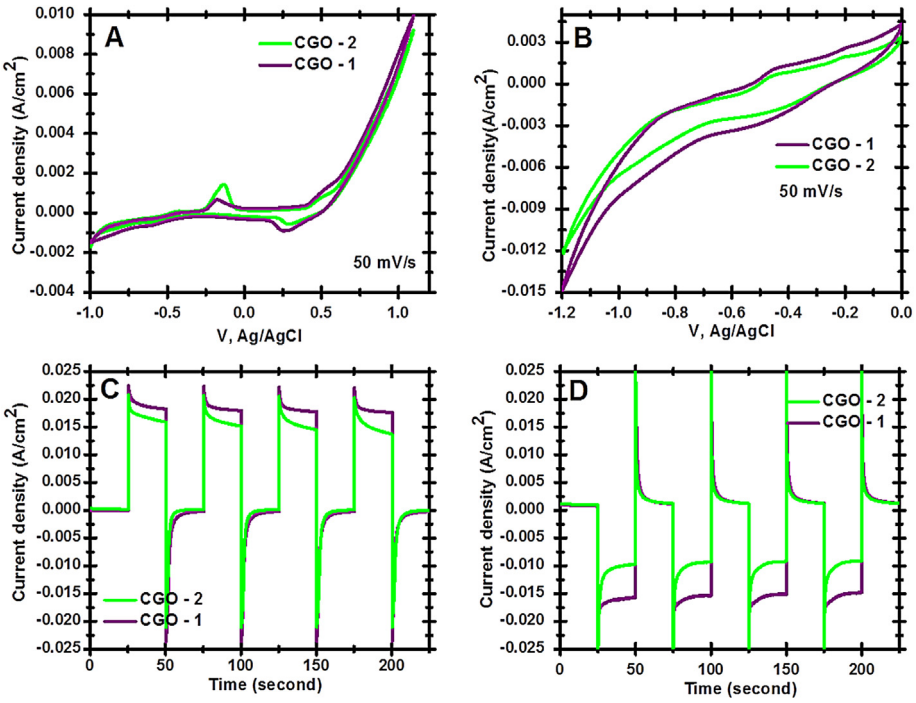

Fig. 4. (a) Cyclic voltammograms (CV) of the nanocrystalline $CuGaO_2$ particles (CGO − 1 and CGO − 2) in 0.5 M KOH by applying the potential range from 1.0 V to −1.0 vs Ag/AgCl with scan rate of 50 mV/s; (b) Cyclic voltammograms (CV) of the nanocrystalline $CuGaO_2$ particles (CGO − 1 and CGO − 2) in 0.5 M KOH by applying the potential range from 0.0 V to −1.2 vs Ag/AgCl with scan rate of 50 mV/s for H_2 generation; (c) Chrono-amperometric (CA) studies of the nanocrystalline $CuGaO_2$ particles (CGO − 1 and CGO − 2) for O_2 generation at 0.6 V with multiple cycles (each cycle for 25 s); (d) Chrono-amperometric (CA) studies of the nanocrystalline $CuGaO_2$ particles (CGO − 1 and CGO − 2) for H_2 generation at 0.6 V with multiple cycles (each cycle for 25 s).

cycles. The current density of the materials depends on the size and morphology of the materials. TEM studies show higher size with agglomeration of the particle of CGO − 2 compared to the particles of CGO − 1. Therefore, the inconsistency in the current density of CGO − 2 could be due to the larger size of the agglomerated particles. Earlier, the current density of delafossites $CuGaO_2$ oxides particles was reported ~8 mA/cm^2 for O_2 generation from the electrolysis of water [2] while the present work here shows that nanocrystalline $CuGaO_2$ particles generate approximately two times higher current densities of ~18 and ~14 mA/cm^2 of CGO − 1 and CGO − 2, respectively, at much lower potential (i.e. 0.60 V). The as − synthesized delafossite $CuGaO_2$ nanoparticles also show better electro-catalytic activity than other reported delafossites (e.g. $CuRhO_2$ [2], $CuFeO_2$ [2] and $CuAlO_2$ [1,2]) for O_2 generation from the electrolysis of water. Fig. 4d shows chrono-amperometry (CA) measurements of CGO − 1 and CGO − 2 to confirm the bifunctional catalytic activity towards the H_2 generation in 0.5 M KOH at the fixed cathodic potential of −1.20 V for 25 s with multiple cycles. CA studies of both electrode materials clearly observe that the CGO − 1 electrode has higher current density than the CGO − 2. The current densities of CGO − 1 and CGO − 2 were found to be around 15 and 10 mA/cm^2, respectively, for H_2 generation. Highly efficient H_2 production using renewable energy will result in lower hydrogen cost. H_2 can be used as a clean fuel in the fuel cells by transforming the chemical energy into electrical energy. Herein, we report that the delafossite $CuGaO_2$ nanoparticles behave as the bifunctional efficient electro-catalyst. The investigation of bifunctional catalytic activity of $CuGaO_2$ nanoparticles for O_2 and H_2 generation could be highly splendid as the next generation fuel.

4. Conclusions

Delafossite $CuGaO_2$ nanoparticles (CGO − 1 and CGO - 2) were synthesized by the sol gel method followed by firing under controlled (N_2 99.99% or controlled $pO_2 = 10^{-5}$ atm) atmospheric conditions at 850 °C. Phase purity of the materials and the average size of the particles (~40 nm) were investigated from PXRD and TEM studies. Moreover, the present work also expressed a significant impact of the $CuGaO_2$ nanoparticles on the clean and renewable source of energy. Delafossite $CuGaO_2$ nanoparticles illustrated the bifunctional electro-catalytic activity to the O_2 and H_2 generation at the anodic and cathodic potentials, respectively, in 0.5 M KOH electrolyte solution versus Ag/AgCl.

Acknowledgements

We are gratefully acknowledged “The Deanship of Scientific Research, Research Center, College of Science,” King Saud University, Kingdom of Saudi Arabia to support this work.

References

[1] J. Ahmed, Y. Mao, Delafossite $CuAlO_2$ nanoparticles with electrocatalytic activity toward oxygen and hydrogen evolution reactions, in: Nanomaterials for Sustainable Energy, American Chemical Society, 2015, pp. 57–72.
[2] R. Hinogami, K. Toyoda, M. Aizawa, S. Yoshii, T. Kawasaki, H. Gyoten, Active copper delafossite anode for oxygen evolution reaction, Electrochem. Commun. 35 (2013) 142–145.
[3] R. Hinogami, K. Toyoda, M. Aizawa, T. Kawasaki, H. Gyoten, Copper delafossite anode for water electrolysis, ECS Trans. 58 (2013) 27–31.
[4] J. Ahmed, C.K. Blakely, J. Prakash, S.R. Bruno, M. Yu, Y. Wu, V.V. Poltavets, Scalable synthesis of delafossite CuAlO2 nanoparticles for p-type dye-sensitized solar cells applications, J. Alloys Compd. 591 (2014) 275–279.
[5] K. Gurunathan, J.-O. Baeg, S.M. Lee, E. Subramanian, S.-J. Moon, K.-J. Kong, Visible light assisted highly efficient hydrogen production from H2S decomposition by CuGaO2 and CuGa1−xInxO2 delafossite oxides bearing nanostructured co-catalysts, Catal. Commun. 9 (2008) 395–402.
[6] M. Yu, G. Natu, Z. Ji, Y. Wu, p-Type dye-sensitized solar cells based on delafossite CuGaO2 nanoplates with saturation photovoltages exceeding 460 mV, J. Phys. Chem. Lett. 3 (2012) 1074–1078.
[7] J.W. Lekse, M.K. Underwood, J.P. Lewis, C. Matranga, Synthesis, characterization, electronic structure, and photocatalytic behavior of CuGaO2 and CuGa1−xFexO2 (x = 0.05, 0.10, 0.15, 0.20) delafossites, J. Phys. Chem. C 116 (2012) 1865–1872.
[8] C. Ruttanapun, Optical and electronic properties of delafossite CuBO2p-type transparent conducting oxide, J. Appl. Phys. 114 (2013) 113108.
[9] M. Han, K. Jiang, J. Zhang, W. Yu, Y. Li, Z. Hu, J. Chu, Structural, electronic band transition and optoelectronic properties of delafossite CuGa1-xCrxO2 (0 [less-than-or-equal] x [less-than-or-equal] 1) solid solution films grown by the sol-gel method, J. Mater. Chem. 22 (2012) 18463–18470.
[10] A. Buljan, P. Alemany, E. Ruiz, Electronic structure and bonding in CuMO2 (M=Al, Ga, Y) delafossite-type Oxides: an ab initio study, J. Phys. Chem. B 103 (1999) 8060–8066.
[11] J. Li, A.W. Sleight, C.Y. Jones, B.H. Toby, Trends in negative thermal expansion behavior for AMO2 (A=Cu or Ag; M=Al, Sc, In, or La) compounds with the delafossite structure, J. Solid State Chem. 178 (2005) 285–294.
[12] X. Nie, S.-H. Wei, S.B. Zhang, Bipolar doping and band-gap anomalies in delafossite transparent conductive oxides, Phys. Rev. Lett. 88 (2002) 066405.
[13] W. Su-Huai, N. Xiliang, S.B. Zhang, Electronic structure and doping of p-type transparent conducting oxides, in: photovoltaic specialists conference, Conf. Rec. Twenty-Ninth IEEE 2002 (2002) 496–499.
[14] T. Omata, H. Nagatani, I. Suzuki, M. Kita, H. Yanagi, N. Ohashi, Wurtzite CuGaO2: a new direct and narrow band gap oxide semiconductor applicable as a solar cell absorber, J. Am. Chem. Soc. 136 (2014) 3378–3381.
[15] H. Kawazoe, M. Yasukawa, H. Hyodo, M. Kurita, H. Yanagi, H. Hosono, P-type electrical conduction in transparent thin films of CuAlO2, Nature 389 (1997) 939–942.
[16] Z. Xu, D. Xiong, H. Wang, W. Zhang, X. Zeng, L. Ming, W. Chen, X. Xu, J. Cui, M. Wang, S. Powar, U. Bach, Y.-B. Cheng, Remarkable photocurrent of p-type dye-sensitized solar cell achieved by size controlled CuGaO2 nanoplates, J. Mater. Chem. A 2 (2014) 2968–2976.
[17] M.-H. Li, J.-H. Yum, S.-J. Moon, P. Chen, Inorganic p-type semiconductors: their applications and progress in dye-sensitized solar cells and perovskite solar cells, Energies 9 (2016) 331.
[18] Y. Kumekawa, M. Hirai, Y. Kobayashi, S. Endoh, E. Oikawa, T. Hashimoto, Evaluation of thermodynamic and kinetic stability of CuAlO2 and CuGaO2, J. Therm. Anal. Calorim. 99 (2009) 57–63.
[19] R. Srinivasan, B. Chavillon, C. Doussier-Brochard, L. Cario, M. Paris, E. Gautron, P. Deniard, F. Odobel, S. Jobic, Tuning the size and color of the p-type wide band gap delafossite semiconductor CuGaO2 with ethylene glycol assisted hydrothermal synthesis, J. Mater. Chem. 18 (2008) 5647–5653.
[20] B. Chavillon, L. Cario, C. Doussier-Brochard, R. Srinivasan, L. Le Pleux, Y. Pellegrin, E. Blart, F. Odobel, S. Jobic, Synthesis of light-coloured nanoparticles of wide band gap p-type semiconductors CuGaO2 and LaOCuS by low temperature hydro/solvothermal processes, Phys. Status Solidi (a) 207 (2010) 1642–1646.
[21] J. Ahmed, C.K. Blakely, S.R. Bruno, V.V. Poltavets, Synthesis of MSnO3 (M=Ba, Sr) nanoparticles by reverse micelle method and particle size distribution analysis by whole powder pattern modeling, Mater. Res. Bull. 47 (2012) 2282–2287.
[22] P. Melnikov, V.A. Nascimento, L.Z. Zanoni Consolo, Thermal decomposition of gallium nitrate hydrate and modeling of thermolysis products, J. Therm. Anal. Calorim. 107 (2011) 1117–1121.
[23] J. Ahmed, S. Vaidya, T. Ahmad, P. Sujatha Devi, D. Das, A.K. Ganguli, Tin dioxide nanoparticles: reverse micellar synthesis and gas sensing properties, Mater. Res. Bull. 43 (2008) 264–271.
[24] B. Kumar, S. Saha, A. Ganguly, A.K. Ganguli, A facile low temperature (350 [degree]C) synthesis of Cu2O nanoparticles and their electrocatalytic and photocatalytic properties, RSC Adv. 4 (2014) 12043–12049.
[25] J. Ahmed, P. Trinh, A.M. Mugweru, A.K. Ganguli, Self-assembly of copper nanoparticles (cubes, rods and spherical nanostructures): significant role of morphology on hydrogen and oxygen evolution efficiencies, Solid State Sci. 13 (2011) 855–861.